The Report committee for Kenneth Avery Perrine
certifies that this is the approved version of the following report:

Design and Implementation of an Underwater Acoustic Transponder

APPROVED BY

SUPERVISING COMMITTEE:

Brian L. Evans, Supervisor

Neal Hall

Design and Implementation of an Underwater Acoustic Transponder

by

Kenneth Avery Perrine, B.S., M.S.

REPORT

Presented to the Faculty of the Graduate School of

The University of Texas at Austin

in Partial Fulfillment

of the Requirements

for the Degree of

MASTER OF SCIENCE IN ENGINEERING

THE UNIVERSITY OF TEXAS AT AUSTIN

May 2011

Acknowledgments

The research described herein was truly a team effort. Many thanks to my colleague and fellow student Karl Nieman who was very much on top of everything pertaining to communications and receivers, Terry Henderson for mentoring that could not be matched anywhere, Keith Lent for wise direction of the project's objectives, and TJ Brudner for inviting all of this project's opportunities.

Design and Implementation of an Underwater Acoustic Transponder

Kenneth Avery Perrine, MSE
The University of Texas at Austin, 2011

Supervisor: Brian L. Evans

A transponder for underwater acoustic data communications is prototyped. The mobile transponder emits a data sequence whenever it detects a ping from a base station. The data sequence includes GPS coordinates and UTC time sent over a conservative and brief 12 kbps turbo-coded BPSK link, and a 6 kB JPEG image sent over an ambitious 67 kbps turbo-coded 16-QAM link. The range of the transponder from the base station can also be accurately derived. Several challenges exist in decoding the underwater signals at the base station receiver, including Doppler distortion and multipath. While experimental results show that the ranges for decoding the 16-QAM signals with a single hydrophone are limited to less than 25 m, the BPSK signals prove to be much more robust, decoding at ranges of up to 625 m. Experiments with delays and transducer tether length indicate methods for improving reliability in the presence of reverberation and thermocline. This transponder uses mostly off-the-shelf parts and is anticipated to be improved when paired with advanced sonar array devices.

Table of Contents

List of Tables

List of Figures

Chapter 1

Introduction

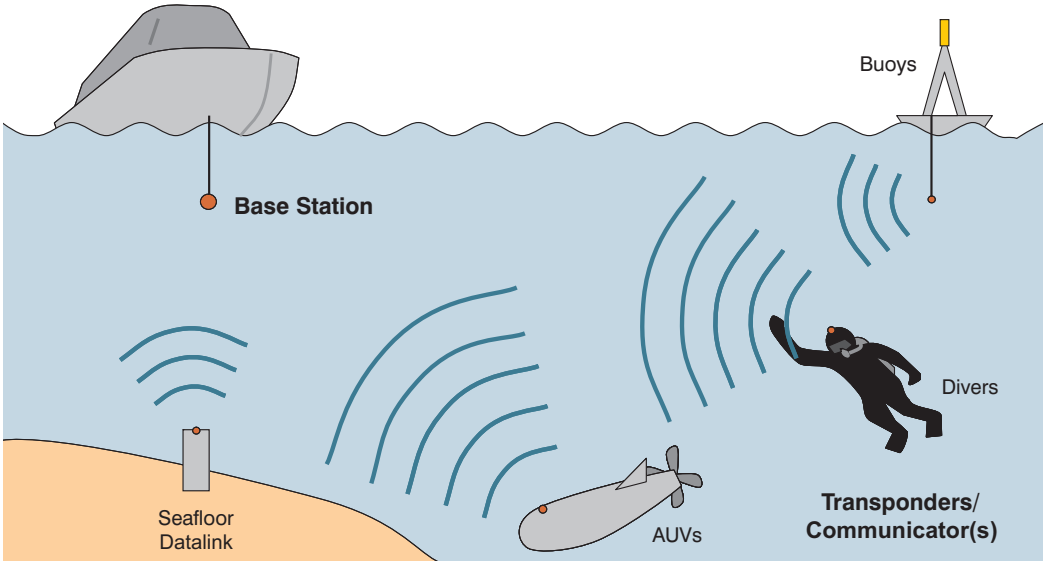

Figure 1.1: Possible scenarios for underwater acoustic transponders.

There is an increasing need to be able to send data wirelessly through water. In open oceans and shallow lakes, several applications exist for data transmission using acoustic communications (ACOMMS), as RF or optical communications attenuate quickly or require too much power. For example, the control of automated underwater vehicles, encoded voice transmissions from divers to a base station, or undersea sensor networks all are prime candidates for ACOMMS. Figure 1.1 shows such scenarios. An element found in many applications is the *transponder*—a de-

vice that is triggered by a signal to emit a response such as a data sequence.

The underwater communications channel presents many challenges in the successful transmission of data, however. Two major problems in ACOMMS include Doppler distortion and multipath reverberation, although other detrimental effects of the underwater channel also exist, such as thermocline, volumetric absorption, and noisy sea life. Indeed, whereas RF systems through air must primarily deal with multipath reverberation through equalization, characteristics of the water medium and the relatively slow speed of sound—5 orders of magnitude slower than the speed of light—make the other challenges especially pertinent.

This report describes the design, construction and performance of a prototype data transponder that sends GPS coordinates and image data whenever it receives a ping from a base station. The transmission of the coordinates and image data involves a single link from one omnidirectional transducer at the transponder to a receiving transducer at the base station. The design is purposefully general-purpose and intended to be evolved to a hardware implementation for different applications such as automated underwater vehicle or diver communications. And, although the prototype incurs considerable latency in its software-based MATLAB implementation, many of its algorithms can be adapted to highly compact and efficient hardware.

This report first elaborates on uses of transponders and the challenges of ACOMMS. Then, focus is given to various solutions for Doppler distortion and multipath reverberation. Next, the methodology for the transponder's design is illustrated, beginning with specific requirements, and proceeding to processing algorithms on both the base station and transponder. Finally, shallow water experimental results are presented that demonstrate the transponder's performance, including data rates and ranges of successfully decoded transmissions.

1.1 Transponder Applications

The purpose of a transponder is to receive some kind of trigger signal and output another signal, perhaps in a different medium. For several fields of scientific research, there have been multiple uses for underwater acoustic transponders.

One purpose is for navigation of automated underwater vehicles (AUVs). A popular navigation technique is called Long Baseline (LBL) [10] [19]. In LBL, three or more transponders are fixed (in a large triangle, for example) in known locations. The AUV emits a ping within the field of the transponders. The transponders then emit a response when they receive the ping, and the AUV receives the responses. Equipment on the AUV then calculates its location with respect to the positioned transponders by evaluating the delay of each response from the time that the initial ping was emitted.

Another use for underwater transponders is to convert underwater signals to RF signals in air. One realization for such a device again involves LBL navigation, but this time combined with the ability to send RF signals to a remote base station [5]. These signals can carry information on an AUV's location, for example. The radio transmitters are mounted on top of anchored buoys and the acoustic transducers hang beneath. It is also possible to use buoys that are free to drift, and to update the known position through the use of GPS, as long as an operable range to the AUV can be maintained within the field of buoys.

The research described in [24] describes the use of transponders that are attached to sperm whales to track the whales' locations. Then, the same hydrophone arrays that are used to roughly identify pods of whales from their natural sounds can also receive acoustic signals emitted from the transponders whenever a ping is issued. In this way, movements of individual whales are known, augmenting the more ambiguous measurements of pod movements. Observations of individual

whale dives in excess of 800 m are reported. The whale transponders are designed to be disposable, as whale tissue replacement typically causes the transponders to be shed at around 12 weeks after tagging.

The transponder system prototyped within this work addresses an application scenario in which a remote diver or AUV is requested via a ping to send information to a base station. This is accomplished by having a sonar at the base station emit a ping that then causes the transponder (attached to the diver or AUV) send back digital data that may include status updates, images, or encoded voice data. Although a single kind of ping from the base station is implemented within this prototype, it is straightforward to envision the use of multiple types of pings, or pings followed by encoded digital data, to pass commands or other kinds of messages to one or more remote divers or AUVs.

Another immediate enhancement to the application scenario involves the use of an array of acoustic receivers that is normally used for acoustic undersea imaging with beamforming [21]. Under normal operation, an imaging system emits a ping and then samples reflections of the pings from remote objects within its field. The array of receiver elements on the imaging system allows it to divide its field into many sectors via beamforming techniques, while range may be derived by the return delay. If a transponder lies within the imaging system's field, the ping can trigger the transponder to send back an active response. This response could then appear much more pronounced than the reflections—distinguishable from the background—but also subject to the same ranging capabilities of the imaging system. Furthermore, the transponder's response could include digital communications that are decoded by processing equipment attached to the imaging system.

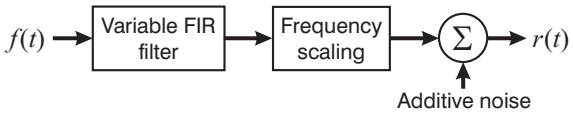

Figure 1.2: This channel impairment model (with f as a perfect signal and r as the received signal) accounts for bulk Doppler distortion with a constant frequency scaling (or offset), preceded by a finite impulse response (FIR) filter with variable complex taps for multipath and time-varying Doppler effects. Impairments not addressed by these two blocks appear as additive noise. This is further explored in Section 2.2.

1.2 Channel Impairments

A variety of likely impairments within the underwater channel can interfere with the successful operation of a transponder. Two major problems, multipath and Doppler distortion, must be specifically addressed in any transponder/receiver design that is to perform ACOMMS with a respectable degree of reliability [16]. The channel model that is ultimately used with this project is shown in Figure 1.2, and further elaborated in Section 2.2. Systems that communicate in a horizontal direction (e.g. where the transmitter and receiver are both at a similar depth) are more suceptible to problems than systems that communicate in a vertical direction (e.g. from the surface to the bottom of an ocean) [9].

Multipath is the presence of multiple instances of a transmission arriving at a receiver because of the existence of multiple communication paths. While ideally a direct path would exist from a transponder to a receiver, strong instances may also arrive via a path that reflects off of the bottom of the body of water, or off of the surface. The distances in each of these paths are likely to vary considerably, and the strongest path may not always be the first received. Moreso, up to 500 ms may elapse in some environments before most of the signal energy reaches the receiver [9] [14].

Doppler distortion is apparent on the direct path when the distance between the transmitter and receiver changes—an occurrence that easily happens between floating objects in water. Additionally, time-varying deflections off of the rippling surface of water or changing currents within water can impose Doppler distortions on some paths. Doppler distortions are much more apparent in acoustic communications than with RF for typical applications because sound waves travel 2×10^5 times slower than the speed of light. As an example, a 50 Hz shift in a 100 kHz center frequency can be apparent in a transponder moving away from a receiver at only 2.7 km/h. Also, because acoustic center frequencies are orders of magnitude lower than many RF communications implementations, an ACOMMS transponder's processing algorithms for, say, a 30 kHz bandwidth must operate with a wideband perspective, whereas an equivalent RF system operating with a much higher center frequency may exercise a number of narrowband assumptions. Doppler distortions cannot be modeled by a simple frequency shift [3] as in narrowband systems; rather, a scaling of frequency in a signal's time-based samples is required because the frequency shift is a function of a continuous range of signal frequencies.

Other channel impairments cause attenuation of a signal as range increases. This acoustic loss is attributed to volume reverberation and absorption imposed by characteristics of water [9]. As shown in [13], absorption is also exponentially increased as frequency of the transmitted signal increases. For example, a 1000 kHz signal undergoes a 40 dB loss over 1 km. In addition to absorption, spherical spreading imposes a loss that increases exponentially as range increases.

A major problem that changes depending upon the season of the year is that of thermocline, the presence of temperature gradients that most often become cooler as depth increases [14]. The changes in temperature alter the sound propagation speed. In typical scenarios, sound propagation paths curve downward. This can

create situations where it is impossible for a direct path to be established from a transponder to a receiver; instead, the only paths are those that reflect off of the bottom of the body of water, or off of the surface.

Various sea life contributes significantly to overall noise levels within oceans. “Many peculiar chirps, grunts, boops, groans, yelps, and barks heard in the sea are of biological origin” [23]. In an analysis of biologically-originated sounds surrounding Australia [2], types of sounds vary greatly, with frequencies ranging from less that 20 Hz with whales to 200 kHz with dolphins and shrimp. Noise levels are found to seasonally and spatially vary. Biological sound sources can be placed into two categories: ongoing background noise, generally of lower frequencies up to 4 kHz, created by colonies or choruses of marine life, and transient sounds, generally of higher frequencies, that significantly exceed background noise. For example, occasional observations of transients exceeded background noise by 30 dB. A notable source of transient noise is snapping shrimp, capable of creating impulsive noise with frequencies that exceed 200 kHz. As an example, interference caused by various sea life moving toward the ocean surface at night is reported in the whale tagging research [24].

Other sources of interference may include other sonar devices within the same vicinity as the transmitter-receiver pair under observation. In a thorough survey on challenges that can affect undersea sensor networks [16], underwater TDMA and CDMA are identified as a means to facilitate coordinated underwater omnidirectional communications that share similar frequency ranges, but with many caveats and limitations due to device power requirements and sound propagation speed. In all cases, the need for wideband communications and the lack of a governing agency as the FCC to regulate frequency usage leads to potential challenges in making a variety of collocated devices successfully operate simultaneously.

As an example, an earlier experiment involving ACOMMS data collection at the Applied Research Laboratories Lake Travis Test Station was delayed by interference from a nearby depth sounder that shared the frequency range of the test waveforms. Because of the loudness of the depth sounder, it was deduced that it would have been impossible to successfully decode most of the affected transmitted waveforms unless the depth sounder was turned off.

In summary, the underwater channel is a complex channel that imposes many impairments for the successful use of transponders. A receiver that can address the strongest impairments (e.g. Doppler effects) specific to locales and conditions (e.g. marine life) exhibits the most reliability and versatility. Because of characteristics specific to acoustics and water, some techniques for RF receiver signal processing cannot be directly applied to ACOMMS [9].

Table 1.1: List of acronyms found in this report and their meanings.

Acronym	**Meaning**
ACK	Acknowledgement (data communications)
ACOMMS	Acoustic communications
API	Application Programming Interface
AUV	Autonomous Underwater Vehicle
BPSK	Binary Phase Shift Keying (method for encoding digital data)
CDMA	Code Division Multiple Access
CRC	Cyclical Redundancy Check (for bit error detection)
CSV	Comma Separated Value (data file format)
Daq	Data acquisition (here, a device for analog/digital input and output)
DFE	Decision Feedback Equalizer
FFT	Fast Fourier Transform (method for acquiring a frequency distribtion)
FIR	Finite Impulse Response
FPGA	Field Programmable Gate Array (a reconfigurable hardware device)
GPS	Global Positioning System
IEEE	Institute of Electrical and Electronics Engineers
JPEG	Joint Photographic Experts Group (lossy image compression format)
LBL	Long Baseline (method for acoustic positioning)
LFM	Linear Frequency Modulation (a “sweep” through frequencies)
MATLAB	Matrix Laboratory (computer language)
MEX	Dynamically linked, compiled subroutine for MATLAB
MISO	Multiple Input, Single Output (related to MIMO, Multiple Input, Multiple Ouptut)
NAK	Negative Acknowledgement (data communications)
NMEA	National Marine Electronics Association
PLL	Phase Locked Loop
PSK	Phase Shift Keying (a family of methods for encoding digital data)
QAM	Quadrature Amplitude Modulation (method for encoding digital data)
QPSK	Quadrature Phase Shift Keying (method for encoding digital data)
RF	Radio Frequency
SNR	Signal to Noise Ratio
TDMA	Time Division Multiple Access
UTC	Coordinated Universal Time
XOR	Exclusive Or (Boolean logic operation)

Chapter 2

Background

Before introducing the design requirements of the transponder and details about its implementation, it is useful to first look at algorithms that allow for successful ACOMMS, specifically in the presence of Doppler distortion and multipath reverberation.

2.1 Transponder

Signals that trigger acoustic transponders are often a linear frequency sweep (LFM) [7]; in LBL navigation for example, additional encoded information beyond the trigger is not necessary [10]. LFM autocorrelation is similar to the autocorrelation of band-limited noise, but also has the notable advantage of being tolerant to Doppler shifts.

It can be necessary, however, to allow transponders to receive and decode digital data, such as for applications where a AUV feeds data to a transponder for reporting purposes, or where multiple AUVs coexist and are simultaneously tracked within a field of transponders [10]. In these cases, it is necessary for the transponder to contain more advanced processing capabilities as described in the next section.

2.2 Receiver

To address two of the most influential forms of channel impairments, multipath reverberation and Doppler distortion, it is helpful to use a channel model as employed in [14] based on linear time t, modeling every received signal $r_i(t)$ through path i from a transmitter to a receiver as:

$$r_i(t) = A_i f((1 + d_i)t - \tau_i) \tag{2.1}$$

where

A_i is an attenuation scaling factor for channel i representing absorption loss and spherical spreading,

$f(t)$ is the transmitted signal,

d_i is the Doppler offset, a scaling factor, and

τ_i is the travel time on path i from the transmitter to the receiver.

Then, if N paths reach the receiver, the total received signal is modeled as:

$$r(t) = \sum_{i=1}^{N} A_i f((1 + d_i)t - \tau_i) + v(t) \tag{2.2}$$

where

$v(t)$ is additive noise.

The results of this model can be reproduced in terms of the Figure 1.2 block diagram.

2.2.1 Doppler Distortion

In a simple model, distortions can be regarded as bulk Doppler that exists throughout the duration of a packet. In this case, in Equations (2.1) and (2.2), d_i remains constant for the entire packet. If this is true, then good correction can be achieved from a single bulk Doppler measurement. A wideband correction can be achieved through involved computations for resampling a waveform. One approach for accomplishing this is to upsample and filter a waveform, and then interpolate it at a new sampling frequency.

One straightforward method for measuring Doppler distortion is to use cross-correlation to identify the locations of expected sequences such as LFMs with a received packet, and to then to compare the distance between the sequences with the expected distance. Contraction or expansion of a waveform would then result in a one-to-one relationship with the difference in distance. A drawback of this technique is that the granularity of detectable Doppler shifts may be too great when cross-correlations are performed on real samples; it may be necessary to oversample the waveform first, which would require more computations and memory usage. It is important to note, too, that the presence of noise in these referenced sequences can cause inaccuracies in the locations of maximum correlations.

A related idea allows a bulk Doppler estimate to be derived from the cross-correlation between two successively repeated symbol sequences [12]. Since the estimation in this work is derived by the phase of the correlation, it is necessary to use basebanded sequences for bulk Doppler detection. This technique is also sensitive to noise, and bears the drawback that the estimate is related only to samples localized to a small area of a much larger packet. Experiments in [17] did not succeed well in the shallow underwater channel.

To guard against the effects of noise, it is helpful to use samples from the

entire duration of a packet in a bulk Doppler estimation scheme. One such technique involves the recovery of a signal's carrier and measuring the carrier's frequency. This is accomplished by raising received samples to a power of 2 (for BPSK) or 4 (for QPSK), taking its Fast Fourier Transform (FFT), and comparing the dominant frequency with the expected frequency. This difference in frequency corresponds with the bulk Doppler correction that is needed. A drawback of this technique is that noise increases in power along with the signal. Another drawback is that it is not feasible to use this technique with modulations of a higher order than QPSK.

In a similar spirit to carrier recovery, it is also possible to encode one or more pilot tones just outside of the frequency range of a signal and observe a shift in frequency from what is expected. Unfortunately, in the underwater channel, such narrowband tones are very susceptible to fading caused by cancellations from multipath, as seen in [17].

Finally, bulk Doppler can be estimated through the use of a replica bank. Upon a receiver's initialization, many copies of a "ground truth" training sequence waveform are created as a *bank*, where each copy is resampled to simulate a possible Doppler distortion. Two parameters that influence the size of the bank are the range of frequency offsets that would be expected and supported within a receiver's environment, and the granularity of frequency offsets. For example, the granularity would need to be fine enough that an equalizer would not be thrown off by residual bulk Doppler remaining after correction is applied. Then, upon each received waveform, the waveform is cross-correlated with each entry in the bank. The frequency offset corresponding with the bank entry that yields the highest cross-correlation result is the most likely to best characterize the bulk Doppler. As can be imagined, a large bank requires many calculations, although it is possible to apply some procedural intelligence to reduce the search space.

As opposed to the simple bulk Doppler model, it is common to see Doppler distortion vary throughout the duration of a packet in transmission. In this case, d_i in Eqs. (2.1) and (2.2) is not constant, as seen in Figure 2.1. This adds a great deal of complexity to computational effort needed to successfully decode a packet. Even so, it is most efficient to remove bulk Doppler before addressing the time-varying Doppler distortion.

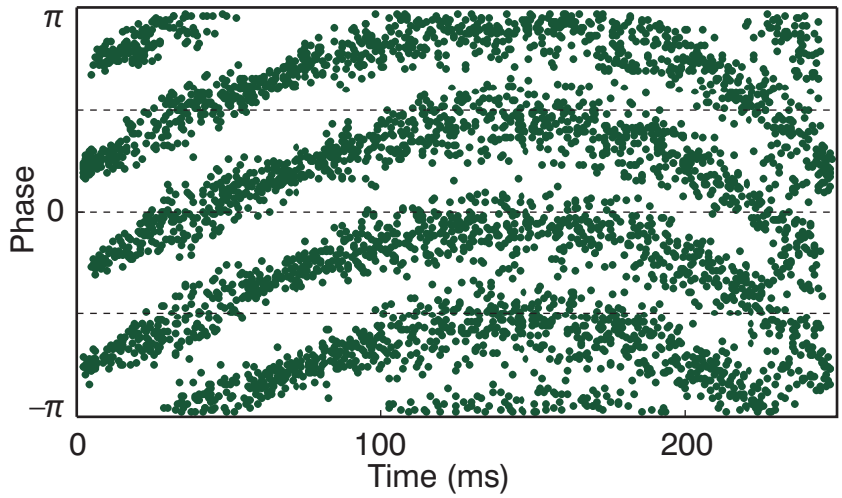

Figure 2.1: Time-varying Doppler effects on a QPSK signal after bulk Doppler correction is applied. Compare the varying phase to the Voronoi regions (delimited by dashed lines) that correspond with the receiver's maximum-likelihood detector. Maximum phase error is apparent at the peak offset near 150ms. Reprinted from [17].

One technique that is helpful for approximating the time-varying Doppler distortion is to use a windowing technique as introduced in [17], where a single packet is divided into a series of partitions. A bulk Doppler distortion estimate is then taken for each partition using, for example, one of the techniques identified earlier in this section. Two caveats exist, however. First, the window size cannot

be so small that, given the presence of noise, the bulk Doppler estimate is poor. Consequences of poor estimates were discovered in [17]. The second caveat is that the joining of bulk Doppler corrected windows can produce abrupt changes (e.g. infinite derivatives) in phase offset at the window edges that can throw off adaptive equalizers.

Without windowing, the phased lock loop (PLL) can be used to track changes in frequency caused by time-varying Doppler distortion [8]. The PLL can track the center frequency of PSK-modulated waveforms but is not as amenable for waveforms of higher modulation. In these cases, it can be possible to track a pilot tone that is coincident with the original waveform. PLLs are, however, difficult to properly configure and maintain for waveforms that undergo significant multipath and severe time-varying Doppler distortion.

It is also possible to leave the removal of time-varying Doppler distortion to an adaptive equalizer. One approach is to incorporate a PLL into the equalizer [11]. An equalizer that has single-tap adaptation exhibits similar functionality as in incorporated PLL, and can be used with waveforms of higher-order modulation than PSK. Also, a fully-adaptive equalizer can be used. Equalization is further addressed in the next section.

2.2.2 Multipath Reverberation

Equalization is a standard technique for addressing multipath reverberation. Two steps in an equalization scheme include channel impulse response characterization and signal correction. Computational complexity of each of these schemes is described in [14].

As practiced in [14] and [17], an equalizer may follow a decision feedback structure where the equalizer's taps are estimated at the start of each received packet

by minimizing the mean squared error over a packet's training sequence. Throughout the duration of processing on the packet, a series of linear operations remove the channel impairments modeled by the initial estimate [8]. Assuming that the channel characteristics had remained constant throughout the duration of the packet, and the training sequence is long enough to allow the channel to be sufficiently characterized, almost all channel effects caused by multipath can be removed.

In reality, however, the underwater channel is very likely to change throughout the duration of a packet. Paths can fade in and out, and time-varying Doppler distortion may exist. It is therefore important to use adaptive equalization [17], such as decision feedback equalization (DFE) [11]. In DFE, both finite and infinite responses can be initialized as noted with static equalizers, but changes in the channel can be discovered and tracked (for example, by comparing the constellation position of a symbol outputted by the equalizer with its closest ideal constellation position) by updating one or more of the equalizer's taps.

A simple adaptive equalizer can include one adaptive tap for the purpose of adjusting the gain and phase of a received signal. As noted above, the phase adjustment is useful for compensating for Doppler distortion, but can also to a certain degree compensate for a strong path that undergoes fading. If, however, a multipath environment exists where different paths fade in and out, it is beneficial to dedicate computational resources to use more than one adaptive tap, as seen in [14].

The channel determines how the equalizer is best configured. In a DFE of any number of feedforward and feedback taps, an important parameter is the adaptation rate—a scaling factor that determines how much of a correction can be applied to each tap at every iteration. Where feedback taps are involved, a high rate of adaptation may make the equalizer susceptible to instability. This parameter may be bounded above to guarantee stability, but such a bound may not allow for

sufficient adaptation rates needed for quickly varying channels [11]. The number of adaptive taps is also an important parameter; too few make the equalizer unable to adapt to necessary changes in the channel, whereas too many make the equalizer respond slowly to changes while incurring a greater computational cost.

Chapter 3

Methodology

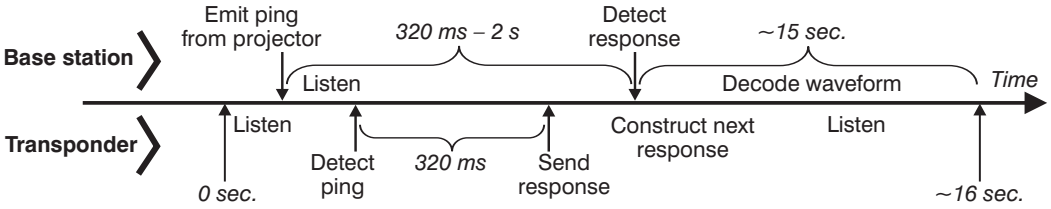

Figure 3.1: Base station and transponder process flow with respect to time.

The complete system described in this report consists of a *base station* and a remote *transponder*. Figure 3.1 shows how the base station and transponder work with respect to time. The base station initiates a communications cycle by emitting a ping. The transponder then hears the ping and responds by emitting a waveform. The base station samples the returned waveform and decodes the data that is encoded therein. It also uses the delay between the ping and the returned waveform to estimate the range, the distance to the transponder. Building off of this framework, this chapter describes the system's design goals and implementation details.

3.1 System Requirements

The goals that influence the design of the system can be divided into two categories. First, there are functional goals. A major goal is to determine whether it is possible for a transponder system as described in this report to work for ap-

plications such as text messaging, command and control, and image request. This influences the function, in that the “round trip time” from the ping to the received packet must exist within a time that facilitates useful interaction; for example, it cannot involve offline post-processing. In addition, the timing between ping output and response reception at the base station must be accurately tracked because transponder range is to be determined from the round trip time, a function of sound speed in water. This inherently requires that the turnaround time from ping receive to response on the transponder is consistent.

Also, the center frequency and bandwidth were chosen around the operational frequencies of the characteristics of the piezoelectric transducers that were available for this project. As a result, a center frequency of 125 kHz was chosen with a bandwidth of 31 kHz. Raw data rates that mostly filled the available bandwidth were selected: 25 kbps (kilobits per second) for BPSK, and 100 kbps for 16-QAM. Furthermore, prior experiences with ACOMMS supported the idea of using an error correcting code, as the probability for bit errors was high at any range [14] [17].

The second category of goals pertains to experimental utility—that is, goals that affect what can be learned from experiments performed with the system. The foremost goal is that the system be easily modified. When the transponder system design was first considered, there was a great deal of thought behind a hardware implementation. Shortly thereafter, the motivation to design hardware gave way to the idea of using hardware only where needed, but to perform most of the processing in software. Furthermore, much of the prior ACOMMS research leading up to this project used MATLAB code. Although MATLAB code is often slower than compiled and optimized C++ code for example, the flexibility available with MATLAB outweighed the need for fast processing.

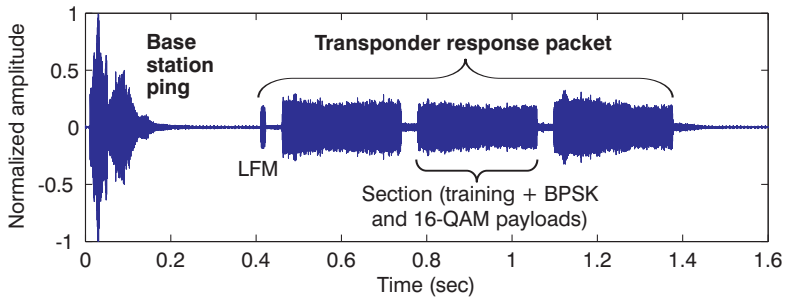

Figure 3.2: Waveforms as perceived by the base station hydrophone. At the time of this response, the transponder was 58 m away from the base station.

The other goal for experimental utility influenced the waveform design for both sides of the system. The base station ping consists of a 20 ms LFM upsweep over the band. The use of the LFM as the ping facilitates the need for less processing power on the transponder because of the LFM's resilience to Doppler distortion. The returned packet then includes an LFM upsweep of 10 ms followed by three sections that are each 275 ms in length, each separated by 40 ms of silence. This is illustrated in Figure 3.2. This scheme was chosen because of previous intuition concerning adaptive equalization and time-varying Doppler distortion; that is, the chance that a DFE becomes unstable increases as packet length increases; hence, the shorter packets. The shorter packets and periods of silence also reduce the chance that reverberation drastically decreases the signal to noise ratio (SNR). In particular, silence allows reverberant build-up during the duration of a packet to partially die off. Finally, each packet includes both BPSK and 16-QAM payloads. The inclusion of both allow for more thorough discovery during experimentation, as the conservative BPSK portion is intended to be received with ranges and channel complications that are far worse than the ambitious 16-QAM portion.

Turbo-codes are used in both of the payloads to provide error correction

[1]. The coding rate on the BPSK portion is 2:1, meaning that for every two bits transmitted, 1 bit is useful data after decoding; and the 16-QAM portion is 3:2 coded. Each portion also includes a 32-bit cyclical redundancy check (CRC) to verify that the turbo-coded portions are successfully decoded. After coding, the payload of the BPSK portion is 24 bytes, and the 16-QAM portion is 3000 bytes.

3.2 Transponder

The transponder includes both hardware and software. The hardware performs input/output of waveforms, data, and images, while the software performs the signal processing for determining when pings are received and for the construction of output waveforms.

3.2.1 Hardware

The central element of the transponder hardware is a 3.0 GHz Intel Pentium 4 PC running Windows XP, with 1 GB of RAM, in a compact Shuttle XPC form factor. Through USB, two devices are attached. The first is a GlobalSat BU-353 GPS receiver, used to obtain GPS coordinates and UTC time. The BU-353 appears within the computer's operating system as a serial port. A MATLAB function is responsible for reading from the serial port and parsing the NMEA (National Marine Electronics Association) GPS device sentences that pertain to coordinate and time updates [20]. The data then appears to the rest of the MATLAB code as three double-precision values; one for GPS latitude in decimal format (where southern coordinates are negative and northern coordinates are positive), one for GPS longitude (where western coordinates are negative and eastern coordinates are positive), and one for UTC time (in which numbers are arranged according to digits, where the first two are hours, the second two are minutes, and the third two are seconds).

The other USB device is an IOTech PersonalDaq/3000 module [4] that features a variety of digital and analog input/output ports and a programmer's API. Of interest to this project are a 16-bit analog-to-digital port for input, and a 16-bit digital-to-analog port for output. Both can be driven at 500 kilosamples per second, and both share a common internally-generated clock. These are associated with circular buffers that can be accessed through the API.

One major concern in the planning phase of the project was the presence of Windows XP and USB in the round-trip chain of events. Both of these technologies notoriously do not operate as real-time systems. In a real-time system, it can be expected that repeated executions of the same process will take the same amount of time. The solution for this is to make the input and output on the Daq operate off of the same clock and then feed the response waveform into the circular buffer at an expected number of samples after the time the ping is detected. Upon rare occasions, the Windows system can be extraordinarily busy, and the software cannot write to the output buffer in time. Fortunately, when this happens, the occurrence is detectable; otherwise the output waveform is emitted consistently at exactly the expected time. All functions for interfacing with the Daq are written in C++ and made accessible to MATLAB through MATLAB's MEX interface.

Another device, a webcam, is attached via the computer's IEEE 1394 interface. The webcam and its interface are configured to generate images at 320x240 resolution in RGB (red, green, and blue) color. Because of the ease of interfacing with Java in MATLAB, a Java class was written to retrieve snapshots from the webcam by interfacing with the Java Media Framework API [15]. The Java class then retrieves the image as a raster object and uses the Java ImageIO facilities to write a JPEG-encoded image to a memory buffer. The JPEG encoding process is iterative, since the combined usable payload among the transponder's three packets

is 6 kilobytes. To achieve this size limitation, the JPEG compression quality setting that affects the quantization of the image's magnitudes in the frequency domain can be reduced to make the resulting JPEG file smaller at the cost of image quality. The class begins attempting to write a JPEG image with a quality setting of 0.5 and then adjusts that value until either 0 is reached (triggering an error condition), or an image that is 6 kB or less in size is written. The memory buffer is then passed to MATLAB in the form of an unsigned 8-bit valued vector.

For acoustic input, a standard Type H52 hydrophone is used [6]. The Type 52's sensitivity is horizontally omnidirectional, concentrated in a 20-degree vertical wedge. This hydrophone is connected to pre-amplifiers that feed into an analog input on the Daq where 16-bit digital samples over a $\pm$10V range are taken at a rate of 500 kilosamples per second.

For output, a 16-bit digital-to-analog output from the Daq is connected to a powered amplifier (a consumer car stereo Polk Audio PA200.4 amplifier that interestingly operates well at our frequency ranges) that is attached to a matching transformer. This causes over 100V to be fed to an output omnidirectional piezoelectric transducer that was manufactured at the Applied Research Laboratories, where about 1W of acoustic energy is placed into the water. The sample rate of the output is 500 kilosamples per second.

Although the hardware is not compact and consists of many parts, it is conceivable that components providing the same functionalities as the existing hardware can be designed and integrated into a compact, custom-designed system. Additionally, a single transducer can take the place of the two currently used by incorporating a transmit-receive switch, an automatically-controlled device that can toggle the role of a single transducer from an emitter to a listener.

3.2.2 Software

The software performs the transponder housekeeping, the ping detection, and the waveform generation. The housekeeping tasks involve initializing the driver to the Daq, opening the serial port to the GPS, and starting the video capture process. In addition, to accelerate later processes, an FFT of the ping is generated and cached in memory. Other caches that are created include the root-raised cosine filter with rolloff factor 0.2 used in the waveform generation, the preamble sequence, and the scrambling code. A log file of the comma-separated value (CSV) format is also created to contain time-stamped information on correlation values and sample indices of pings.

The software that interfaces with the Daq is then configured to operate in *blocks* of 20 kilosamples, or $\frac{20 \text{ kilosamples}}{500 \text{ kilosamples/sec}} = 40 \text{ ms}$ increments. Given the need to perform cross-correlation on successive pairs of blocks to match incoming pings, it was found that the circular buffers were ideally configured to contain 4 input blocks and 3 output blocks. This results in latency between signal reception and transmission of $\frac{(4+3) \times 20 \text{ kilosamples}}{500 \text{ kilosamples/sec}} = 280 \text{ ms}$. If the number of blocks used for the circular buffers is reduced, the latency is reduced, but the probability of the software skipping an incoming block or missing the window for the outgoing block greatly increases. This skipping behavior is a drawback of the Daq's limited programmer API features and hardware characteristics. Although a production transponder system would ideally incur far less latency, this prototype system performed consistently with the given buffer configuration and was therefore suitable for testing purposes.

A loop begins where a new block is read from the circular buffer when it is available and then placed into the upper half of a buffer that holds 2 blocks. Then, before the next block is read, the upper half of the buffer is copied to the

lower half. By using this two-half scheme, pings that extend beyond the end of one block can be successfully matched in their entirety. After each update to the buffer, a frequency domain normalized cross-correlation is performed against the cached ping replica. (It is noted that slightly more efficiency could be realized if an overlap-add method were used.) The maximum correlation that exceeds 0.25 is regarded as a match, and the time index corresponding with the maximum is stored. This allows the output waveform to be positioned within the circular buffer so that it will consistently output at a particular delay after the incoming ping was sampled.

For waveform generation (see Figure 3.3), subsections of the final waveform are created and then joined together. First, an LFM upsweep across the band over 10 ms is generated to facilitate the ability for the base station receiver to identify the start of the packet. After a 40 ms gap, three sections of the general payload waveforms follow, each separated by 40 ms of silence. These gaps are intended to reduce inter-packet interference.

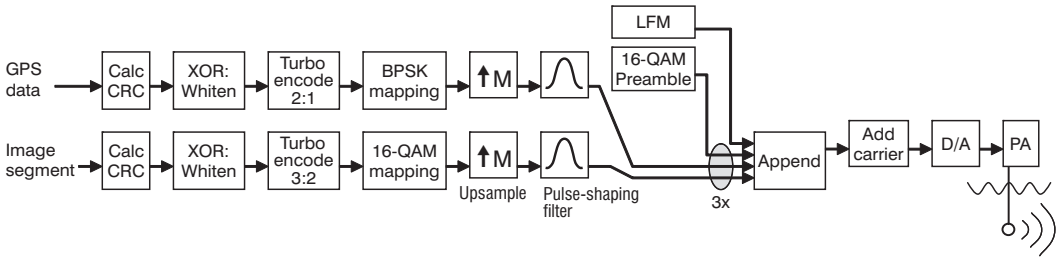

Figure 3.3: Waveform generation structure used on the transponder.

The waveforms include both BPSK symbols and 16-QAM symbols; the BPSK symbol mapping is achieved by using two opposing corners of the 16-QAM mapper. Each section contains a 16-QAM preamble of 512 pseudorandom symbols, a 2:1 turbo coded, BPSK modulated header of originally 12 bytes that includes a

CRC-32 code for the header, and then a 3:2 turbo coded general-purpose, 16-QAM modulated area of originally 2000 bytes with a CRC-32 code. (CRC-32 codes are consistently used because of the convenient availability of a standard Java class that generates CRC-32 codes). The usable bit rate is 12.5 kbps for the BPSK portion and 66.7 kbps for the 16-QAM section. While the header contains GPS latitude, longitude, and UTC time, the 16-QAM payload contains a third of the JPEG image. Prior to turbo-coding, the bit sequence is XORed with a pseudo-random whitening bit sequence. The motivation behind whitening is to balance the spectral energy of the transmission regardless of the spectral content of the input data. This helps the signal be resilient to frequency selective fading and gives the signal moderate security from unwanted listeners.

3.3 Base Station

As with the transponder, the base station includes hardware and software elements. Although the hardware is no more complicated than that found on the transponder, the processing requirements for software are much greater because of waveform decoding tasks.

3.3.1 Hardware

The central element of the base station is a 2.67 GHz Intel Core 2 Quad PC running Windows 7 32-bit with 4 GB of RAM. Attached via USB is another PersonalDaq/3000 and GPS device. The Daq performs analog to digital conversion, while the GPS is present as a means to keep timestamps synchronized for logging purposes.

It is conceivable that the digital to analog output of the Daq plus a powered

amplifier setup can be used to emit a ping. In actuality, this was not true for the experiment described in this report. Instead, in the experiment, the ping was originated from a separate sonar projector device that was collocated with the receiver H52 hydrophone. The projector placed an estimated 15.8 kW of acoustic energy into the water. This was horizontally omnidirectional in an approx. 7 degree vertical wedge. This projector operated autonomously, and triggered the base station computer to sample for the waveform coming from the transponder. The reason for this separation and the use of the projector came from project objectives that specified some of the equipment that was used in testing.

3.3.2 Software

The software on the receiver performs several initialization tasks similar to the transponder. Specifically, the Daq driver is opened, the GPS serial listener is started, and both the ping replica and root-raised cosine filter are generated, as well as the replica bank for the bulk Doppler detector.

When the base station receiver is triggered, 3 sec. of samples are retrieved at a rate of 500 kilosamples per sec. from the circular buffer. At this point, the receiver software begins its work. The receiver is structured similar to what is described in [17], consisting of a frame synchronizer, a bulk Doppler detector, a bulk Doppler compensator, and a DFE. In addition to the prior work, a turbo decoder and CRC checker follow the DFE. Also, the receive chain is repeated three times after the initial frame synchronizer to decode the three sections. Figure 3.4 shows the entire receive chain.

The first step in the receiver is frame synchronization. The beginning of the transponder's LFM is discovered through normalized cross-correlation of received samples with the resident replica. A maximum normalized cross-correlation that

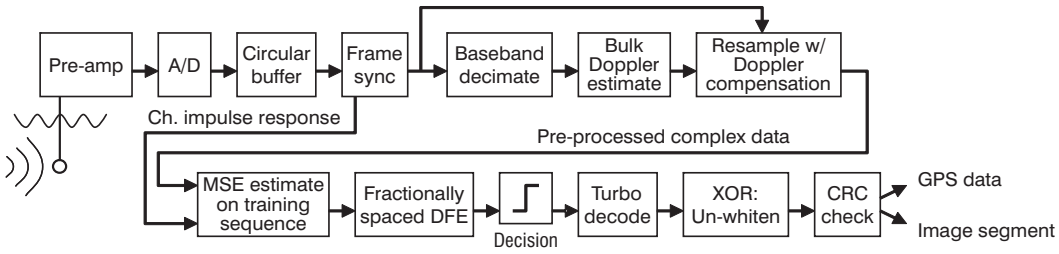

Figure 3.4: Receive chain structure used at the base station.

exceeds 0.25 is deemed a positive match. This match sample position is compared against the time of the initial trigger from the projector; from this, the range of the transponder can be determined according to:

$$L = \frac{C}{2}(D - P) \tag{3.1}$$

where

L is range in m, and

D is the delay from the base station's ping emit to the base station's sampling of the transponder's LFM,

P is the transponder processing time between ping receive and waveform transmit, and

C is the speed of sound in water, approx. 1480 m/s.

The received signal is basebanded and decimated to twice the symbol rate. The remainder of the receive process is repeated three times to decode the three sections. For each section, a secondary frame synchronization is performed by a replica bank bulk Doppler distortion detection, as frame-sync and Doppler detection functions are both facilitated by the cross-correlation mechanism within the

detector. Therein, each replica of the preamble that had been pre-shifted in frequency is cross-correlated with a corresponding section of the received samples. The maximum correlation corresponds with the beginning of the preamble in the received sample and also the closest bulk Doppler offset frequency available within the replica bank. The basebanded waveform is then resampled to compensate for the bulk Doppler. After resampling, a phase correction factor is multiplied in to restore phase information to each sample.

Now, the training sequence is used to initialize a fractionally-spaced DFE (twice the symbol rate) with a least squares solution. This initial solution allows most multipath and residual Doppler distortion at the beginning of the sequence to be undone and decoded. The DFE is configured with 25 forward taps and 10 decision feedback taps; on each successive symbol, these are updated with a DFE adaptation rate of 0.0035. Although it is possible to incorporate turbo-decoding into the equalizer to enhance overall performance [22], this kind of implementation was not performed for this experiment.

After equalization, the decisions are unscrambled using a XOR operation with the same whitener random bit sequence as used on the transponder. Then, the unscrambled bits are turbo-decoded in attempts to eliminate bit errors incurred in the channel and the decoding process. Upon decoding, a CRC-32 is generated and compared with that appearing in the respective decoded section. If the CRC-32 codes match, the respective bits are deemed accurate; if they do not match, then the section's bits are discarded. In either case, the success or failure of each section is logged.

If any of the BPSK sections are successfully decoded, the encoded GPS coordinates and UTC time are displayed, along with the range estimation that was derived from the delay. Then, if all three of the 16-QAM sections are successfully

decoded, the three sections of 2,000 bytes are appended together and passed to a JPEG image decoder. The image is then displayed in a window.

3.4 Data Collection

Applied Research Laboratories experiments in ACOMMS were conducted on July 6, 2009 [14] and Nov. 6, 2009 [13] [17], as well as other times. One of these experiments allowed for the creation of a 5.1 GB publicly released dataset [18]. These experiments lead up to the design of the transponder and the experiment whose results are reported in Chapter 4. All major tests were conducted at the Applied Research Laboratories Lake Travis Test Station.

The lake on which the station floats provides a challenging shallow water environment for ACOMMS. First, the lake is formed over an old river channel; its former rocky ravine and surrounding hilly landscape create a great deal of multi-path. Second, a concrete hydroelectric dam 600 m away from the station provides a very strong sound reflection. Third, during warmer seasons, the thermocline can significantly affect sound propagation and impair long-range communications. It is suspected that all of these problems would not be as apparent in a deep-water ocean environment.

The experiment with the transponder was performed on March 16, 2011. The projector and base station receiver were placed in the test facility, while the transponder on a research vessel was positioned at 11 different locations away from the receiver, as seen in Figure 3.5 and listed in Table 3.1. At each location, the transponder's two transducers were lowered into the water, and pings were emitted from the projector at the base station. On that day, the lake was up to 44 m deep.

At the furthest ranges, it was expected that successful communications would

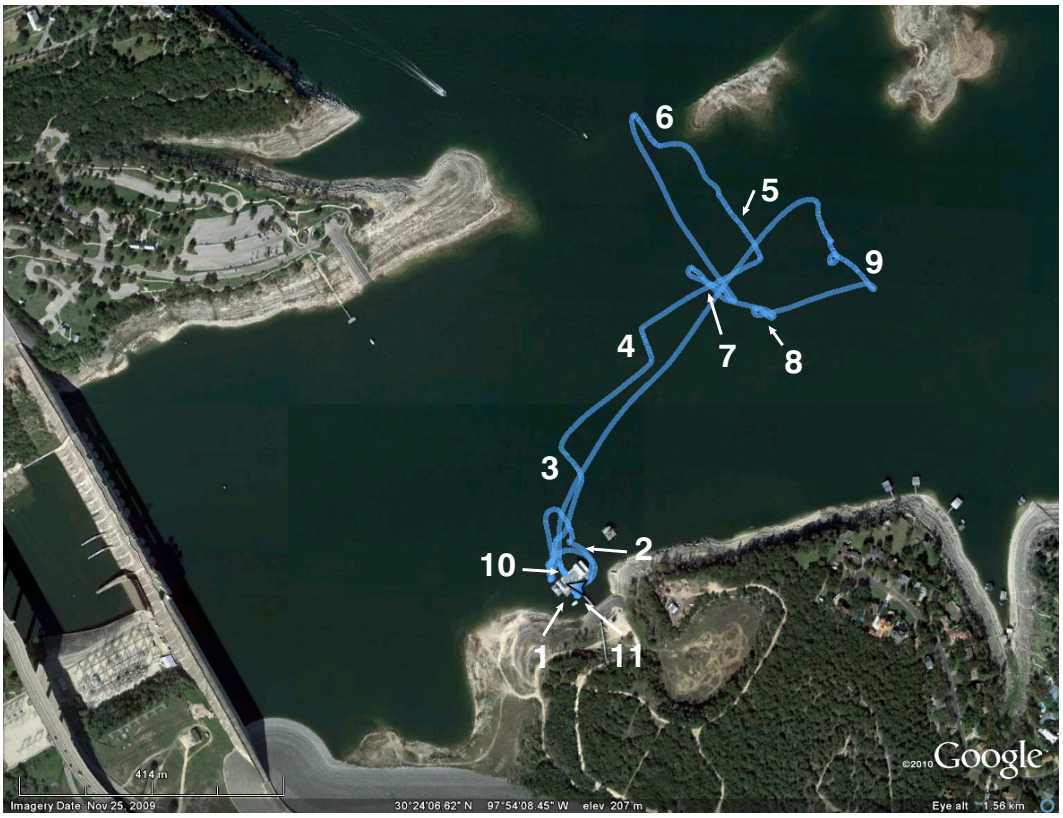

Figure 3.5: Research vessel GPS track with corresponding data collection positions. See Table 3.1 for details on each position.

tail off because of the thermocline prediction raytrace, shown in Figure 3.6. This warranted a test with the transducers at the transponder end placed deeper into the water. Another experiment was conducted where the delay between the ping and the returned waveform was lengthened. The rationale for this was to increase the SNR by waiting until most of the reverberations from the initial ping had died away.

Table 3.1: Research vessel positions for data collection. Note that range varies at some positions because of the boat drifting.

Pos.	**Range**	**Motion**	**Tether**	**Delay**
1	10 m	Docked	6 m	320 ms
2	40 m	Free-floating	6 m	320 ms
3	155-200 m	Free-floating	6 m	320 ms
4	355-390 m	Free-floating	6 m	320 ms
5	558-580 m	Free-floating	6 m	320 ms
6	663-697 m	Free-floating	6 m	320 ms
7	490 m	Free-floating	6 m	320 ms
8	490 m	Free-floating	6 m	320 ms
9	625 m	Free-floating	6 & 18 m	320 ms
10	30 m	Docked	6 m	320 ms
11	10 m	Docked	6 m	900 ms

3.5 Metrics

Logs of events, such as positive matches to pings and their correlation values, are written on both the base station and the tranponder ends. In addition, the base station records the received samples for later analysis and also creates an estimate of SNR for each of the three sections. The SNR estimate at the DFE output is given by:

$$SNRest = 20\log\left(1 \Big/ \sqrt{\frac{1}{N}\sum_{n=1}^{N}|R_n - V_n|^2}\right) \tag{3.2}$$

where

R_n is the nth received symbol, possibly offset by additive noise,

V_n is the nth symbol in the training sequence, positioned directly on a constellation point, unaffected by noise, and

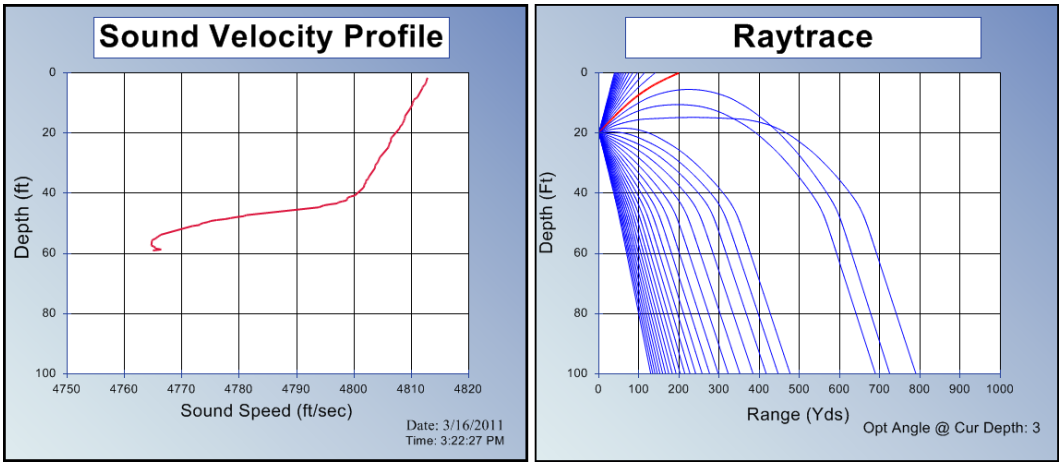

Figure 3.6: Sound velocity calculation and predicted sound propagation caused by thermocline for Mar. 16, 2011 at 3:22 PM. These plots are based upon data taken from temperature sensors placed on a vertical line in the water. Notice that no line-of-sight shallow communications (e.g. less than 20 feet deep) are predicted to be possible at ranges in excess of 600 feet.

N is the number of symbols in the training sequence, 512.

It is important to note that the SNR estimate is based only on the training data found in the preamble of each packet's three sections. This estimate therefore does not represent loss of SNR due to time-varying Doppler distortions, impulsive noise, and other detrimental effects that develop after the preamble's transmission.

Measurements used for analysis include the SNR estimate, indicator values corresponding with successful packet decoding for each of the received BPSK and 16-QAM sections (realized through CRC checks), and range estimates derived from round trip return time. These measurements are also paired with range derived from GPS coordinates.

Chapter 4

Experiment

The data collection activities described in the previous chapter allow for the analysis of three aspects of the transponder prototype and its environment. First, the success rate of transponder-to-base station communications and respective SNR for each response allows the range of the system (given the lake's environmental conditions on the test day) to be characterized. Second, the effects of reverberant noise caused by intrapacket interference of the response can be studied. Third, the ranging capability offered by the measurements that are used in Equation 3.1 can be compared with ranges derived from GPS coordinates measured at both the base station and the moving transponder. Beyond these three points, the data that was collected also brings about the ability to guide the design of future experimental methods.

4.1 Response Success

Figure 4.1 shows the success rate of transponder transmissions back to the base station for both the BPSK and QPSK portions, as well as the SNR estimated off of the training sequence. The points shown represent only pings that were sent from the base station that were received by the transponder. The points are sorted by range derived from the sound speed method described in Section 3.3.2.

Key observations include the expected loss of SNR as range increases. Also,

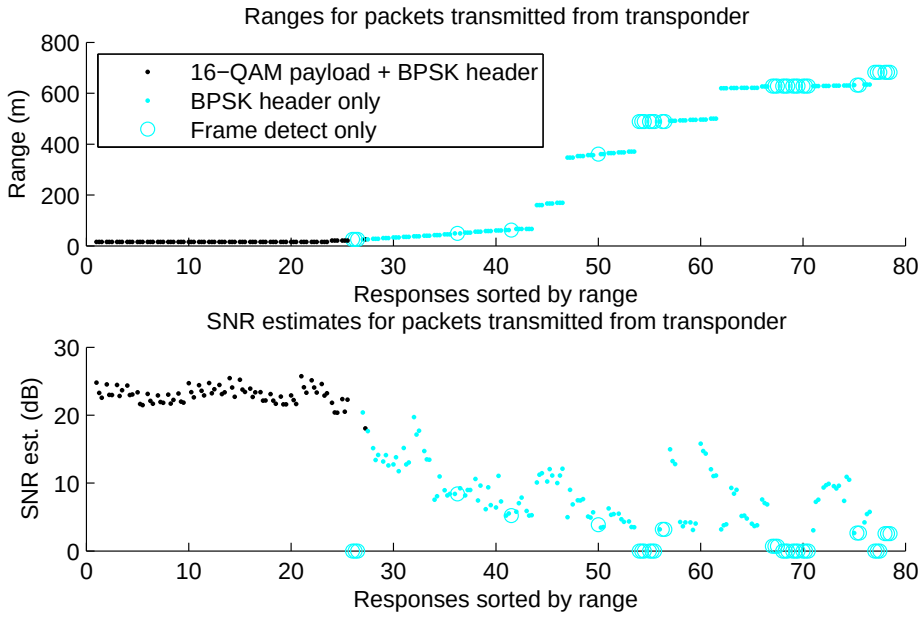

Figure 4.1: Decode successes, ranges, and corresponding SNR values for packets returned by the transponder. Note that points are in sets of three for each packet, where each point corresponds with one of the three sections of each packet.

it is clear that the BPSK portion is much more resilient to range than the ambitious 16-QAM portion. Indeed, the utility of the 16-QAM portion is rapidly lost when the small range of $\sim$25 m is exceeded.

Support for the consistent success of the BPSK sections includes the low SNR requirements for BPSK modulation and the high coding rate. It is also important to note, too, that the packet structure largely prevents time-varying Doppler distortions or other channel effects from interfering with the BPSK section. First, the BPSK section is very short—only 24 bytes after coding. Also, the BPSK section occurs immediately after a sizeable training sequence. These factors offer the best equalizer performance and practically do not require any adaptation within the

equalizer.

In attempts to increase the reliability for far-range communications, the transducer tether length was increased from 6 m (20 ft) to 18 m (60 ft) only while at Position 9, in an impromptu experiment for establishing a direct path given the effects of thermocline at the ∼625 m range. As seen in Figure 4.2, the receive rate for BPSK sections improves at the greater teather length. It must be noted, however, that additional data points would best be collected in similar conditions for these results to be statistically significant.

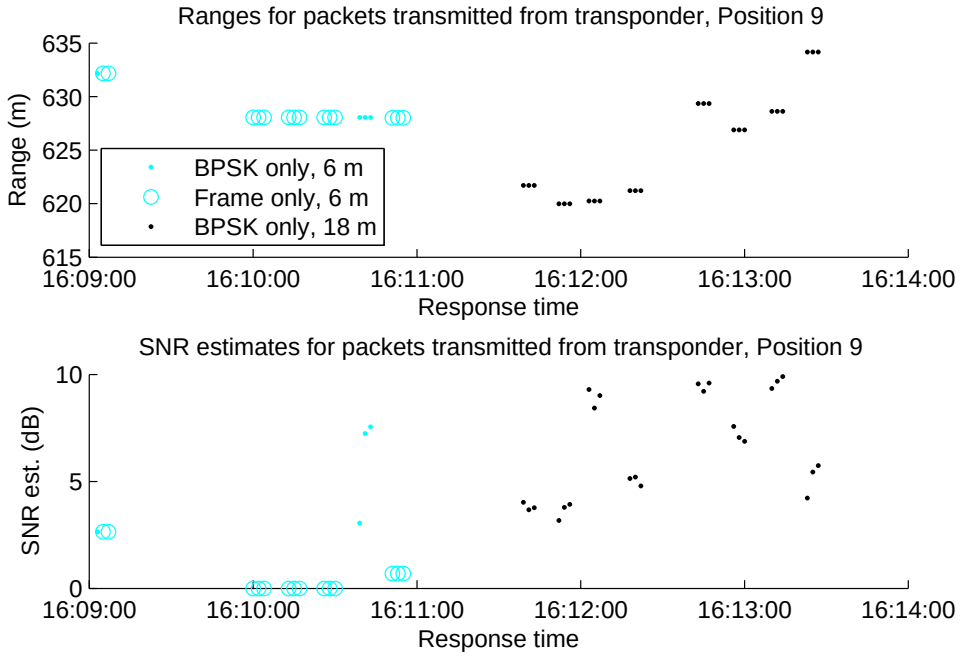

Figure 4.2: A preliminary indication of the influence of transducer depth for the ∼625 m range, Position 9.

4.2 Reverberant Noise

There were indications that reverberant noise caused by the build-up of acoustic energy noticeably decreased the SNR. Two sources of such interference include the comparatively loud ping from the projector at the base station, and intrapacket interference.

An experiment was conducted midway throughout the duration of Position 11 to look specifically at the effects of the reverberant energy from the base station projector's ping on the transponder's signal. On all tests leading up to Position 11, the transponder was configured to transmit its response at exactly 320 ms after the time that the initial base station ping was received. (Recall that this delay allows for Daq buffering, pattern matching, and output waveform placement). Then, this delay was extended to 900 ms with the intent of allowing reverberations from the initial ping to die down. Figure 4.3 shows a side-by-side comparison of the SNR values; in general, SNR is improved by about 3 dB. Caution should be given to this conclusion until further tests are conducted; between Positions 1 and 11 (docked at the same location) over 1 hour elapsed, and transducer locations may have changed by a few centimeters.

Additionally, intrapacket interference can readily be observed (assuming the hypothesis above is true) by closely inspecting Figures 4.1 and 4.3 and noticing that most sets of three successive portions in each response decrease in SNR. (Recall that the graphs are not plotted to time; there are 40 ms gaps of silence between each section within each packet). This successive drop in SNR may be attributed to the idea that the 40 ms gaps do not usually prevent the increase of overall reverberation.

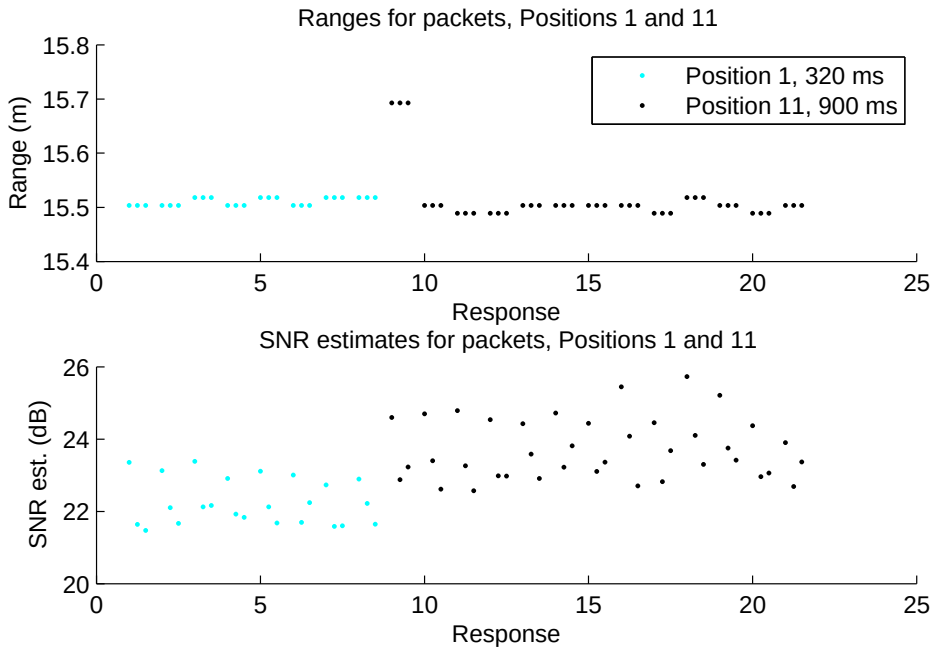

Figure 4.3: Improvement of SNR when transducer turnaround delay is changed from 320 ms to 900 ms.

4.3 Ranging Capability

As explained in Section 3.3.2, range is a function of delay and sound speed in water. A useful test to determine the accuracy of the implementation of this ranging method is to discover its difference from range determined by GPS coordinates from GPS receivers at the moving transponder and the fixed base station. Figure 4.4 shows this difference. Note that 11 data points from those shown in Figure 4.1 had been removed because of GPS device read errors at the transponder. Figure 4.3 hints at the sub-meter consistency of ranges provided by the sound speed measurement technique, whereas it is assumed that accuracy with the GPS equipment is within a few meters.

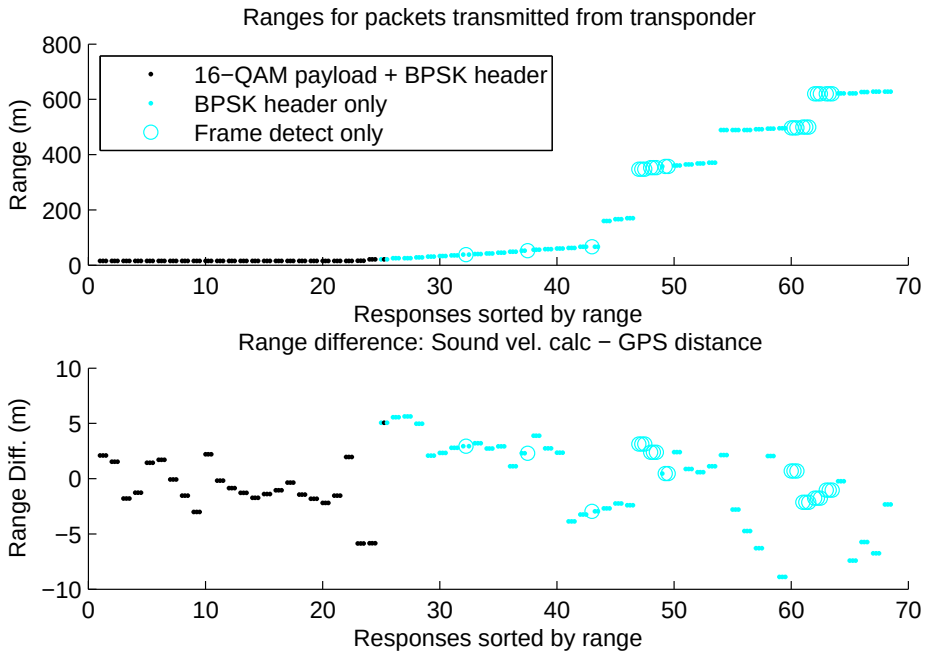

Figure 4.4: Difference in range between the sound delay and GPS difference methods at a subset of test points.

Thermocline has the capacity to alter the range estimation capabilities of the system. In particular, the use of round-trip delay to measure distance does not directly match distance between entities on the lake surface. Instead, it measures the signal path as taken in the water, including the downward curve as seen at further distances. In cases where the dominant signal is one that bounces off of an indirect object, the signal path is arguably longer than a line-of-sight path as seen with GPS.

4.4 Other Findings

Two other measurements would have been ideal to analyze and report, but the methods for conducting the experiment did not adequately afford the ability to make repeatable conclusions. First, it would have been valuable to determine the detection success rate of pings from the base station projector to the transponder. However, data was not collected that allowed for precise knowledge of when the transducers on the boat were lowered into the water and when the base station equipment was operational. For this to be successful, it would be necessary to log the times that these events happen. As it was, it is reasonable to suspect that pings were detected with about a 90% reliability at Positions 1-4 and 10-11, with consistent failure at far ranges such as Position 6 when line-of-sight was not possible because of thermocline or the lake bottom.

Second, with the data that was collected, it is difficult to know how many responses from the transponder to the base station were actually attempted. This arises from a technical problem with the receiver software and its operation with the independent projector, complicated by the lack of time-log data already described. Specifically, the projector's ping rate had about the same period as the time necessary for the receiver to complete its detection and decoding operations; that is, filling the Daq sample buffer, discovering the projector's triggering ping, recording 3 seconds of samples, running the receiver software, and writing the samples to disk. It is apparent that at perhaps 30% of the time, this process may have lasted longer than the projector's ping period, resulting in the base station receiver software "dropping" a packet until the next ping is received. It is suspected from the pattern of missing packets that a lengthening in the ping rate for the projector or further optimization of the receiver code would resolve this problem.

Chapter 5

Conclusion

When this project was commissioned, it was clear that it would bear a first-generation prototype nature. Indeed, one of its purposes was to prove that it was possible to incorporate ACOMMS capabilities into a transponder-like functionality using methods that followed from prior work [13] [14] [17]. Another purpose was to determine future directions that the prototype design could take.

5.1 Key Results

Despite a variety of necessities for a more reliable ACOMMS transponder system, the work reported here offers an encouraging start. First, it has been shown that a mixture of data rates can be achieved in underwater communications despite challenges inherent in the shallow water channel. Doppler distortion and multipath interference has been consistently mitigated for distances up to around 600 m on a day that thermocline was especially prominent. A very short, but repeatable 12 kbps communications path was demonstrated alongside a 66.7 kbps path, although the high-speed path was limited to ranges of less than 25 m.

Second, general-purpose transducers and off-the-shelf equipment were used in this project. The data acquisition items were all parts that could be ordered on-line, and the computation resources included PCs and MATLAB. A rough estimate on the total cost of equipment for the entire transponder system (if it were to use

a lower cost piezoelectric receiver element than the H52 standard hydrophone) is $5000. Cost of labor-hours in software and receiver research is more difficult to quantify, as much of the work placed in the receiver, for example, comes from the sporadic efforts of a small team over the course of over one and a half years.

Finally, this project is instrumental in increasing the awareness of ACOMMS capabilities among those in sonar development research areas. New capabilities can potentially be instilled within existing devices that were never initially designed for ACOMMS. One example is undersea acoustic imaging devices. It is conceivable that changes in software can enable such capabilities without the need for expensive and time-consuming hardware modifications.

5.2 Future Work

As implied in Section 4.4, there were fundamental aspects of the experiment that could be enhanced by collecting a broader range of data (specifically, more time-stamped events), a greater amount of data, and resolving problems with the receiver that were not discovered until the day of the experiment. This would allow a more complete range of performance metrics to be characterized, such as the success rates for the detection of pings from the base station to the transponder.

Since the transponder system's design was made to be general, it is logical to adapt the transponder to other sonar devices than the transducers that were used in this experiment. Logical candidates for new devices include sonar devices equipped with large receiver arrays, allowing MISO (multiple input, single output) to increase SNR, as well as allowing the use of techniques as beamforming and monopulse to selectively direct the sensitivity of the receiver to emitters of interest. Recent work in [13] can be readily adapted to a transponder system, and it is believed that the

use of arrays can dramatically improve the success rate of the higher-speed data capabilities.

Another improvement that would be necessary for a reliable ACOMMS transducer is a mechanism for two-way communications that would allow the base station and transponder to discover thresholds for reliable performance in a given channel. The experimental results showed that reliability was high for the slow BPSK-encoded data, attributed to the nature of BPSK, the shortness of the BPSK section, and the immediate proximity to the training data. It is reasonable, then, to design a system that would use highly coded BPSK for the worst channels—a consistent performance base—and then dynamically use higher speeds for purposes that do not require as great of reliability. As seen with communications at far ranges, it would also be ideal to use an ACK/NAK scheme to allow lost packets to be re-transmitted.

A final improvement would be hardware implementation. Once algorithms are finalized and operational capabilities are known through experimentation, two major benefits can arise from the design of hardware. First, the parallel nature of various hardware as FPGAs can afford faster algorithms than what can be achieved using general-purpose computing platforms. Second, the size and power requirements of a hardware platform would allow the transponder to be placed on AUVs or equipped on divers in ways that are not feasible with a PC. Hardware implementation can be an involved process, but is significantly motivated by the demonstrated capabilities of the proof-of-concept prototype.

Bibliography

[1] C. Berrou and A. Glavieux. Near optimum error correcting coding and decoding: turbo-codes. *IEEE Transactions on Communications*, 44(10):1261–1271, October 1996.

[2] D. H. Cato. The biological contribution to the ambient noise in waters near Australia. *Acoustics Australia*, 20(3):76, 1992.

[3] M. Chitre, S. Shahabudeen, L. Freitag, and M. Stojanovic. Recent advances in underwater acoustic communications and networking. In *Proc. IEEE OCEANS*, pages 1–10, Sept. 2008.

[4] Measurement Computing. Personal Daq/3000 Series. `http://www.mccdaq.com/products/pdaq3s.htm`, last accessed March 28, 2011.

[5] N. Cruz, L. Madureira, A. Matos, and F. L. Pereira. A versatile acoustic beacon for navigation and remote tracking of multiple underwater vehicles. In *Proc. IEEE OCEANS*, volume 3, pages 1829–1834 vol. 3, 2001.

[6] United States Navy Underwater Sound Reference Division. Type H52 Hydrophone, August 1994. `http://www.navsea.navy.mil/nuwc/newport/usrdiv/transducers/H52.pdf`, last accessed March 30, 2011.

[7] M. R. Ducoff and B. W. Tietjen. *Radar Handbook*, chapter Pulse Compression Radar, pages 8.3–8.11. McGraw-Hill, 3 edition, 2008.

[8] C. R. Johnson and W. A. Sethares. *Telecommunication Breakdown*. Prentice Hall, 2004.

[9] D. B. Kilfoyle and A. B. Baggeroer. The state of the art in underwater acoustic telemetry. *IEEE Journal of Oceanic Engineering*, 25(1):4–27, Jan. 2000.

[10] J. Kinsey, R. Eustice, and L. Whitcomb. Underwater vehicle navigation: recent advances and new challenges. In *Proc. IFAC Conf. on Manoeuvring and Control of Marine Craft*, September 2006.

[11] D. G. Messerschmitt and E. A. Lee. *Digital Communication*. Kluwer Academic Press, 1988.

[12] P. H. Moose. A technique for orthogonal frequency division multiplexing frequency offset correction. *IEEE Transactions on Communications*, 42(10):2908–2914, Oct. 1994.

[13] K. F. Nieman, K. A. Perrine, T. L. Henderson, K. H. Lent, T. J. Brudner, and B. L. Evans. Wideband monopulse spatial filtering for large receiver arrays for reverberant underwater communication channels. In *Proc. IEEE OCEANS*, pages 1–8, September 2010.

[14] K. F. Nieman, K. A. Perrine, K. H. Lent, T. L. Henderson, T. J. Brudner, and B. L. Evans. Multi-stage and sparse equalizer design for communication systems in reverberant underwater channels. In *Proc. IEEE Workshop on Signal Processing Systems (SIPS)*, pages 374–379, October 2010.

[15] Oracle. Java SE Desktop Technologies: Java Media Framework (JMF) API. `http://www.oracle.com/technetwork/java/javase/tech/index-jsp-140239.html`, last accessed March 28, 2011.

[16] Jim Partan, Jim Kurose, and Brian Neil Levine. A survey of practical issues in underwater networks. *SIGMOBILE Mob. Comput. Commun. Rev.*, 11:23–33, October 2007.

[17] K. A. Perrine, K. F. Nieman, T. L. Henderson, K. H. Lent, T. J. Brudner, and B. L. Evans. Doppler estimation and correction for shallow underwater acoustic communications. In *Proc. 43nd Asilomar Conference on Signals, Systems and Computers*, November 2010.

[18] K. A. Perrine, K. F. Nieman, K. H. Lent, T. L. Henderson, T. J. Brudner, and B. L. Evans. The university of texas at austin applied research laboratories nov. 2009 five-element acoustic underwater dataset. `http://users.ece.utexas.edu/~bevans/projects/underwater/datasets/index.html`, last accessed April 25, 2011.

[19] S. Singh, M. Grund, B. Bingham, R. Eustice, H. Singh, and L. Freitag. Underwater acoustic navigation with the whoi micro-modem. In *Proc. IEEE OCEANS*, pages 1–4, September 2006.

[20] SiRF Technology, Inc. NMEA Reference Manual, January 2005. `http://www.sparkfun.com/datasheets/GPS/NMEA%20Reference%20Manual1.pdf`, last accessed March 28, 2011.

[21] J. L. Sutton. Underwater acoustic imaging. *Proceedings of the IEEE*, 67(4):554–566, April 1979.

[22] M. Tuchler, R. Koetter, and A. C. Singer. Turbo equalization: principles and new results. *IEEE Transactions on Communications*, 50(5):754–767, May 2002.

[23] R. Urick. *Principles of Underwater Sound*. Peninsula, 3 edition, 1996.

[24] W. A. Watkins, M. A. Daher, K. M. Fristrup, T. J. Howald, and G. N. Di Sciara. Sperm whales tagged with transponders and tracked underwater by sonar. *Marine Mammal Science*, 9:55–67, 1993.

Vita

Kenneth A. Perrine grew up in Tacoma, WA. He started computer programming with an Apple II in 4th Grade and selling a math game while in middle school. He attended Pacific Lutheran University, graduating with a computer engineering degree in 1998, where he experienced the beginning of the desktop video editing revolution. After that, he worked at Pacific Northwest National Laboratory as a research scientist/engineer in a variety of fields, including parallel computing, massive data visualization, image analysis, and usability. In 2007, he sought to return to school and explored a longtime interest in transportation systems, finishing with a MS degree in civil and environmental engineering at University of Washington in 2008. After an internship with City of Seattle in traffic management, he continued school, this time in electrical and computer engineering at University of Texas at Austin in the communications and networking systems track. His research activities at UT have been in underwater ACOMMS and high-speed digital radio at the Applied Research Laboratories. Although his background has been diverse, he has always enjoyed finding connections between sciences and believes that interdisciplinary approaches to problem-solving yield the best and most interesting solutions.

Permanent e-mail address: `kperrine@utexas.edu`

This report was typed by the author.